



*Conference Proceedings Paper – Entropy*

## Grading entropy and degradation of sands and rocks

J. Lőrincz<sup>1</sup>, E. Imre<sup>2,\*</sup>, P. Q. Trang<sup>3</sup>, S. Fityus<sup>4</sup>

<sup>1</sup> Tengizchevroil, Farnborough, Hampshire, United Kingdom

<sup>2</sup> Obuda University, Budapest, Hungary

<sup>3</sup> Geotechnical and Eng. Geol. Department, BME, Budapest, Hungary.

<sup>4</sup> School of Engineering, The University of Newcastle, Callaghan Australia

\* Author to whom correspondence should be addressed; E-Mail: imreemok@gmail.com

*Published: 17 November 2015*

---

**Abstract.** The connection between the grading entropy path and the directional properties of natural or spontaneous processes is investigated in the ongoing research. In this paper some earlier results are reanalysed to study the final state of the breakage process. Breakage tests can be divided into two categories, being the tests with continuous topology and the tests where the continuous topological effects are repetitively disrupted during breakage. Nearly all tests display jumps of the normalised entropy path when the number of fraction present increases, due to the discontinuity of the normalised entropy map, which drifts the path onto the stable part of the normalised entropy diagram. All tests end here, with a final grading curve having an almost fractal distribution. The discontinuous topology tests may reach the theoretical ultimate state if the fraction number stabilises.

Keywords: grading entropy; breakage; sand; compaction

---

### 1 INTRODUCTION

The connection between the grading entropy concept and the directional property of the particle breakage process is analysed on the basis of the results of some breakage tests and some theoretical analyses. In this paper the final state of the breakage process is considered, using the breakage tests results of Lőrincz et al., (2011), Brandl (1977) and Coop et al (2004), as well as some theoretical results regarding the fractal dimension of optimal grading curves and the discontinuity of the normalised entropy map. In the first part of the paper, theoretical results are presented and completed. In the second part the test results are re-analysed.

## 2 GRADING ENTROPY

### 2.1 Definitions

The relative frequencies of the fractions  $x_i$  ( $i = 1, 2, 3 \dots N$ ) of a grading curve satisfies:

$$\sum_{i=1}^N x_i = 1, \quad x_i \geq 0, \quad N \geq 1 \quad (1)$$

Equation (1) defines an  $N-1$  dimensional, closed simplex  $\Delta$  (which is the generalised  $N-1$  dimensional analogy of the 2 dimensional triangle or, 3 dimensional tetrahedron) if the relative frequencies  $x_i$  are identified with the barycentre coordinates of the simplex points. The grading entropy  $S$  has two parts:

$$S = S_0 + \Delta S \quad (2)$$

where  $S_0$  is called the base entropy and  $\Delta S$  is the entropy increment. The base entropy is

$$S_0 = \sum x_i S_{0i} = \sum x_i i \quad (3)$$

where  $S_{0i}$  is entropy of the  $i$ -th fraction which just integer  $i$ . The normalized base entropy is

$$A = \frac{S_0 - S_{0\min}}{S_{0\max} - S_{0\min}} \quad (4)$$

where  $S_{0\max}$  and  $S_{0\min}$  are the entropies of the largest and the smallest fractions, respectively. The entropy increment  $\Delta S$  is

$$\Delta S = -\frac{1}{\ln 2} \sum_{x_i \neq 0} x_i \ln x_i. \quad (5)$$

which varies between 0 and  $\ln N / \ln 2$ , depending on the fraction number  $N$ . The normalized entropy increment  $B$  is

$$B = \frac{\Delta S}{\ln N} \quad (6)$$

The fraction limits are defined by using the integer powers of the number 2 (Lórinicz et al., 2005).

### 2.2 Entropy diagrams and optimal grading curves

Two maps can be considered for a fixed  $N$ : the non-normalized entropy map  $\Delta \rightarrow \mathfrak{R}^1 \times \mathfrak{R}^1$ ,  $\Delta \rightarrow [S_0, \Delta S]$  and the normalized entropy map  $\Delta \rightarrow [A, B]$ . These are differentiable on the open simplex and can continuously be extended to the closed simplex. The images – the entropy diagrams – are compact, like the simplex. Therefore, there is a maximum and a minimum  $B$  value for each fixed  $A$  value.

It can be proved that the function is one-to-one at the maximum bounding line (Imre et al. 2009). The following - so-called optimal grading curve, or optimal point of the simplex, with fixed  $A$  maps on the maximum  $B$ :

$$x_1 = \frac{1}{\sum_{j=1}^N a^{j-1}} = \frac{1-a}{1-a^N}, \quad x_j = x_1 a^{j-1} \quad (7)$$

where parameter  $a$  is the root of the following equation :

$$y = \sum_{j=1}^N a^{j-1} [j-1 - A(N-1)] = 0. \quad (8)$$

The equation of finite fractal distribution (Einav 2007) is

$$F(d) = \frac{d^{(3-n)} - d_{\min}^{(3-n)}}{d_{\max}^{(3-n)} - d_{\min}^{(3-n)}} \quad (9)$$

where  $d$  is particle diameter,  $n$  is fractal dimension. Taking into account that in the grading entropy theory the fraction limits are defined by using the integer powers of the number 2, it can be derived that the relative frequencies of the fractions  $x_i$  ( $i = 1, 2, 3 \dots N$ ) are as follows:

$$x_j = x_1 a^{j-1} \text{ where } x_1 = \frac{(2^{(3-n)} - 1)d_{\min}^{(3-n)}}{d_{\max}^{(3-n)} - d_{\min}^{(3-n)}}, a = 2^{(3-n)} \text{ or } n = 3 - \frac{\log a}{\log 2} \quad (10)$$

It follows that the optimal grading curves have finite fractal distribution: the fractal dimension  $n$  varies between 3 and  $-\infty$  on the  $A > 0.5$  side as  $a$  varies between 1 and  $\infty$ ;  $n$  varies between 3 and  $-\infty$  on the  $A < 0.5$  side of the maximum normalized entropy increment line, as  $a$  varies between 1 and 0. The fractal dimension  $n$  depends on  $N$  (Tables 1, 2) except at the symmetry point of the diagram ( $A = 0.5, B = 1/\ln 2, n = 3, a = 1$ ).

**Table 1.** Table 2 The  $A$  coordinates for a fixed fractal dimension  $n = 2$  (and  $a=2$ ), in the function of  $N$

$N$ [-]	2	3	4	5	6	7
$A$ [-]	0.667	0.714	0.756	0.790	0.819	0.843

**Table 2.** Table 4 The fractal dimension  $n$  for a fixed  $A (= 2/3)$  in the function of  $N$

$N$ [-]	2	3	4	5	6	7
$n$ [-]	2	2.25	2.40	2.49	2.56	2.62

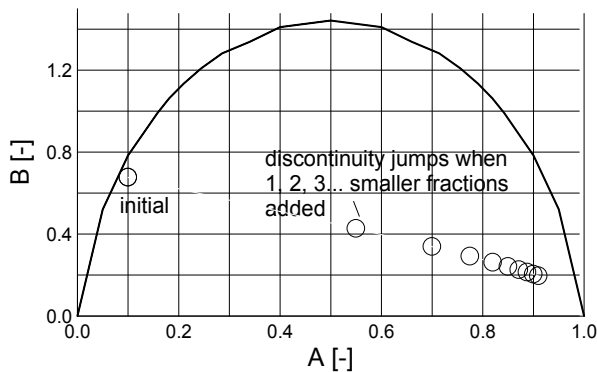
### 2.3 The discontinuity for the normalized diagram

If  $N$  varies, the two maps can still be considered. However, the only the non-normalized entropy map  $[\Delta, N] \rightarrow [S_0, \Delta S]$  is continuous, the normalized entropy map  $[\Delta, N] \rightarrow [A, B]$  is not continuous. Some formulae were derived for the discontinuity. If some zero fractions are added from the smaller side (Lőrincz et al., 2011, Fig 1) then

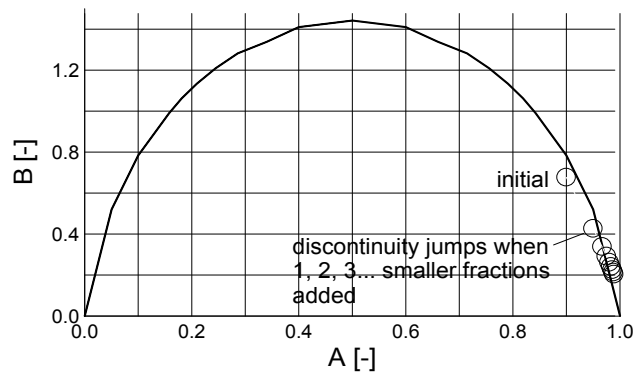
$$B(N) - B(N+i) = \Delta S(N) \frac{1 - \frac{\ln N}{\ln N + i}}{\ln N} \quad (11)$$

The  $A$  change for  $i=1, 2 \dots$  additional smaller zero fractions, respectively is:

$$A(N+i) - A(N) = \frac{i[1 - A(N)]}{N+i-1} \quad (12)$$



(a)



(b)

**Figure 1.** (a) Computed discontinuity in the normalized entropy diagram for an initially  $N=2$ ,  $A<0.5$  optimal soil. (b) Computed discontinuity in the normalized entropy diagram for an initially  $N=2$ ,  $A>0.5$  optimal soil.

### 3 REANALYSED MEASURED DATA

#### 3.1 Reanalysis of some tests with discontinuous topology

The following testing procedure was developed (Lőrincz et al. 2005, 2011) to study particle crushing phenomena. A sample was subjected to a series of crushing treatments using a specially reinforced crushing pot. After the compression, the sample was removed from the crushing pot (disrupting the topology) and the grading curve for the crushed sample was determined by sieving. The sample is then returned to the crushing pot for the further compression. Initially single fraction soils showed a monotonic normalized entropy path, with  $A$  decreasing as  $B$  increased. Some initially multi-fractioned soils silica and carbonate soil mixtures with  $A<0.5$  (Figure 2) showed a significant jump at the start of the test when some new smaller fractions appeared. After this jump, the path continued on the  $A>0.5$  side of the normalised diagram as shown in Figure 3.

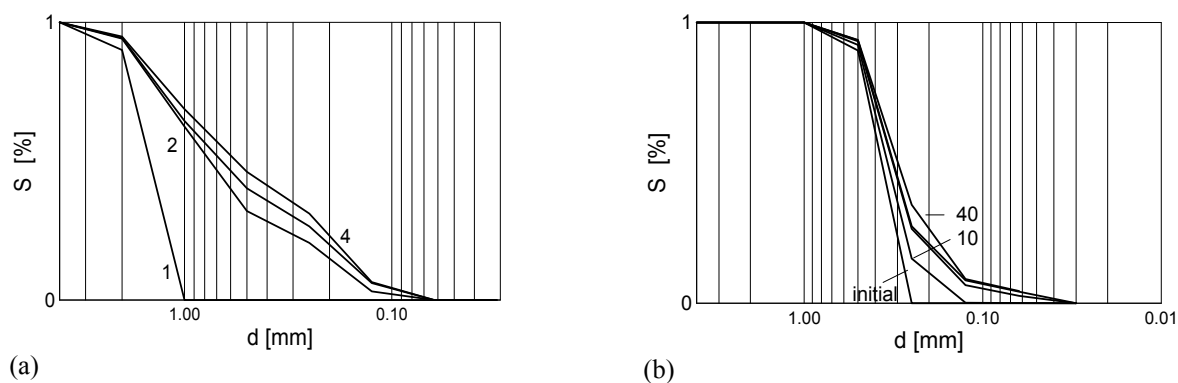


**Figure 2.** Grading curve variation of initially multi-fraction soils. (a) Carbonate sand. (b) Silica sands.

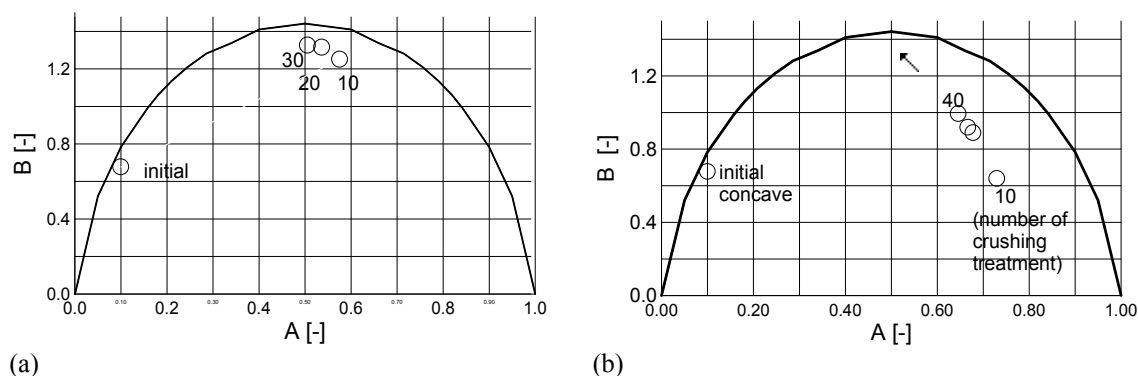


**Figure 3.** Normalised entropy path of initially multi-fraction soils (a) Carbonate sand. (b) Silica sands.

#### 3.2 Tests with continuous topology

Brandl (1977) presents the results of an investigation of particle disintegration of natural sandy gravel and crushed stone bedding courses due to *in situ* compaction and the action of construction traffic. The work also includes a method to predict the disintegration behaviour of these materials, on the basis of simple laboratory investigations. In another series of tests, the effect of freeze-thaw cycles on the load bearing characteristics was investigated, emphasizing the role of fine content of these materials.

Some of the results of the original work are presented in Figure 4 as mean grading curves or as envelopes of the grading curves for the tested soils, before and after treatment. The base entropy  $[A]$  and entropy increment  $[B]$  values for these grading curves have been calculated (e.g., Lőrincz et al. 2005) using some simplifications (e.g., instead of 13-14, only 11 fractions were taken into account). In these figures curve 1 is related to the state after compaction and curve 2 is related to the state before compaction. According to the results, the relative base entropy  $A$  may increase or decrease as a result of the treatment, but the normalised entropy increment  $B$  increases generally.

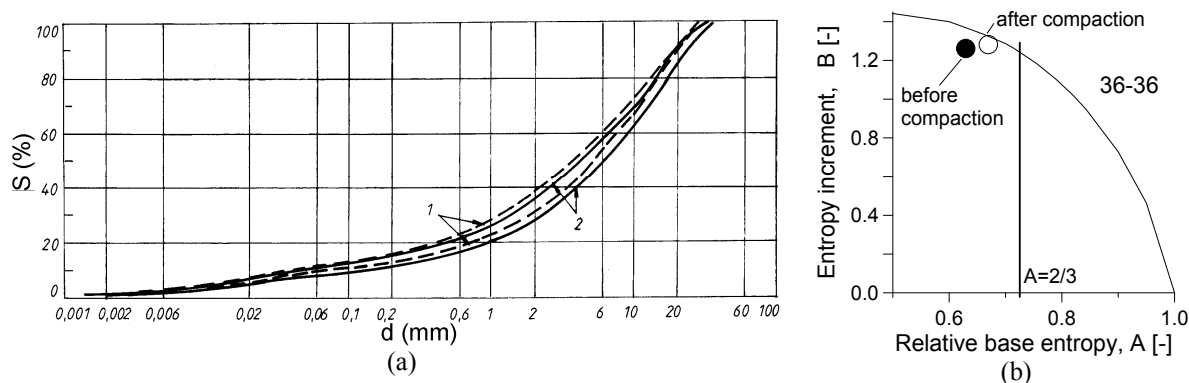


**Figure 2.** Analysis of the grading curves shown in Figure 36 in the work of Brandl (1977). (a) detail of the grading curves (lower and upper envelopes,  $S$  is the percentage passing). (b) entropy diagram related to the lower envelope

*Reanalysis of the shear box tests of Coop et al*

A series of ring shear tests was conducted to investigate the development of particle breakage with shear strain for a carbonate sand. It was found that at very large displacements the soil reached a stable grading. The final grading was not generic, but dependent on both the applied normal stress and the initial grading.

Two typical test results are shown in Figure 5 and Table 3. One starts from a single-fraction and its  $B$  increases. The other starts from a 3-fraction state and its  $B$  decreases. The final (critical) state and theoretical ultimate state (the maximum point of the upper bound line) are relatively far apart in terms of  $A$ . This can be attributed to the fact that the continuous topological effects are not broken (the soil is not remixed). The closest optimal points have increasing finite fractal dimension between 2.4 and 2.8.

**Table 3.** Shear box test data ( $N_{\text{final}} = 12$ ) and the fractal dimension of the closest optimal point

Sample State	Rs3 (Initial grading 0.300–0.425)		Rs8 (Initial grading 0.063–0.425)	
	Initial	final	initial	final
$A$ [-]	1	0.744	0.640	0.669
$B$ [-]	0	1.224	1.361	1.298
$S_0$ [-]	13	10.18	12.28	9.36
$\Delta S$ [-]	0	3.042	1.495	3.225
$n(A,N)$ [-]	$-\infty$	2.62	2.37	2.76

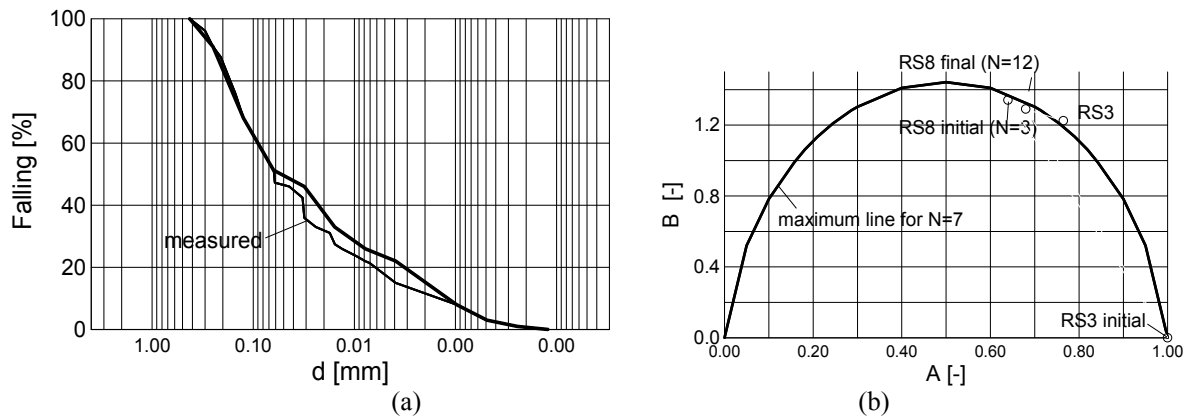


**Figure 3.** Coop's results on Carbonate sands (a) RS8 final grading (measured and transformed for the grading entropy computations). (b) Normalised entropy path.

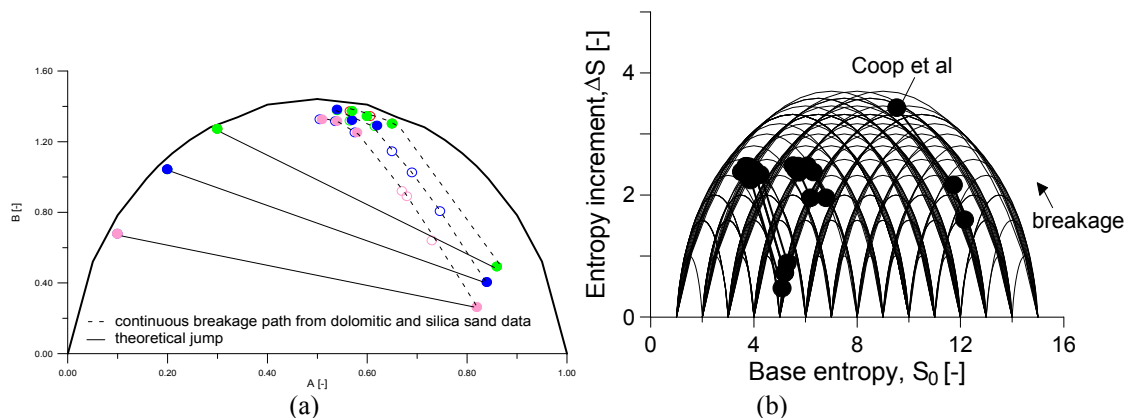


**Figure 4.** (a) The similarity of the normalised breakage paths. Open circles indicate silica sand, full circles carbonate sand, the solid lines indicate the jumps. (b) The non-normalised breakage paths.

#### Analysis of the shear box tests of Dun (2014)

Dun (2014) undertook direct shear tests on identical samples of dry granular rock fill material composed initially of particles from 4 fractions ranging from 19mm to 4.75mm, under 5 confining stresses from 10 to 3500kPa. Two rock types were tested, a weak rock (siltstone) and a strong rock (andesite). The particle distribution of each test sample was pre-determined prior to testing in order to create a baseline value. After testing, the particle distribution was measured to determine the grading changes due to particle breakage.

Two tests were carried out at each confining stress; a test in which samples were subject to compression only test and a second test where a new sample was subjected to both compression and

shear. The compression-only test allowed an estimation of the proportion of particle breakage due to imposition of the confining stress only. This proportion could then be subtracted from the amount of particle breakage for the compression and shear test, to estimate the amount of particle breakage generated by shearing only.

The results of the tests show that, as normal stress increases, there is a decline in the shear strength (peak friction angle) and an increase in particle breakage. The test results for the strong rock (andesite) had similar friction angles to siltstone at very low and very high normal stresses, but showed a higher strength at intermediate stress values. This extra strength was attributed to the ability of the andesite to resist particle breakage up to higher stresses than the siltstone. The experimental evidence in this study supports the hypothesis that particle breakage results in a reduction in the shear strength of dry granular materials.

The entropy paths for the compression-only and compression and shear tests are shown in Figure 7. Interestingly, the initial grading of the samples tested plotted close to the apex of the entropy figure. The breakage due to loading caused a large jump in the entropy path, characterised by a significant decrease in the  $B$  value, and a significant increase in the  $A$  value. Figure 7b implies that the creation of smaller fractions is the main mechanism for the initial change in the entropy value, but that increasing particle damage from higher confining stresses causes the  $B$  value to recover to an increasing extent with increasing load.

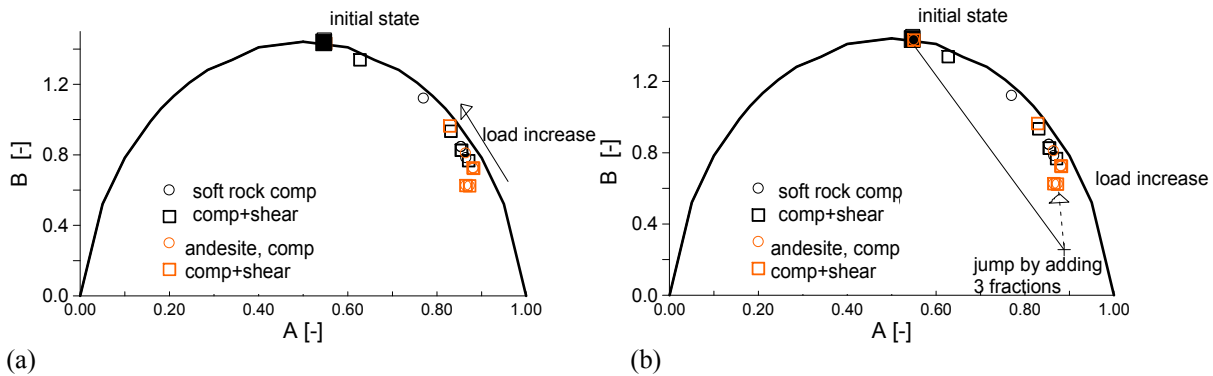


**Figure 5.** Comparison of the normalised entropy paths for weak and strong rock with the same initial grading. (a) The similarity of the normalised breakage paths. Orange symbols indicate silica andesite; black symbols, soft rock. The starting point is the same. (b) The normalised breakage paths indicating the computed jump with solid line.

## 4 DISCUSSION

### 4.1 Entropy path

During breakage the number of the fractions is increasing, but the largest fraction is not vanishing due to the ‘cushioning effect’ of smaller particles. The base entropy  $S_0$  decreases (since the mean diameter decreases), the entropy increment  $\Delta S$  (and the ‘disorder’) strictly monotonically increases during breakage.

The normalized entropy path follows about the same pattern if the number of fraction remains constant during breakage, the relative base entropy  $S_0$  decreases (since the mean diameter decreases), the normalised entropy increment  $B$  (and the ‘disorder’) strictly monotonically increases.

However, temporarily a different, ‘opposite’ path if the number of the fractions changes. The size of the measured ‘discontinuity’ is directly related to  $1 - A$ , being zero if the starting point is a single fraction with  $A = 1$ , in accordance with the suggested formula. The reduction of the mean grain diameter, and the appearance of some finer fractions, may cause a sudden increase in  $A$ .

Physically, the relative base entropy  $A$  (the weighted mean of the reduced fraction entropies) is related to the stability of the grain structure, without any knowledge on the actual geometrical setting, according to the finding of Lőrincz (1986). The grain structure is unstable if  $A$  is less than  $2/3$ . The reduction of the mean grain diameter, and the appearance of some finer fractions, may cause a sudden increase in the stability of the grain structure.

## 4.2 Uniqueness of Entropy path

The normalised entropy path is the same for the same “normalised” initial grading curve (i.e. the size of the smallest fraction is indifferent). This is a new result, which can be used to develop a new geological test compiling hardness and brittleness properties.

There is a significant difference in the rate of breakage of the silica and the carbonate sands, which is also evident in the andesite and siltstone gravels, where the latter in each case is much weaker.

The breakage tests can be divided into two categories; into tests with continuous topology; and into the tests where the continuous topological effects are repetitively disrupted during breakage. In the first category the path can be shorter than in the case of the tests with discontinuous topology.

## 4.3 Final state

The results concerning the final state of the normalised particle breakage paths can be summarized as follows. If the path starts from a single fraction case ( $A=1$ ) then it follows the maximum  $B$  line. Therefore, the final state of a test with continuous topology – at the moment when the critical state is attained – seems to be an optimal grading curve state represented by a point on the maximum normalized entropy increment line, on the  $A>0.5$  side of the normalized entropy diagram.

The optimal grading curves have finite fractal distribution, the fractal dimension  $n$  varies between 3 and  $-\infty$  on the  $A>0.5$  side,  $n$  varies between 3 and  $-\infty$  on the  $A<0.5$  side of the maximum normalized entropy increment line. These depend on  $N$  except at the symmetry point of the diagram ( $A = 0.5, B = 1/\ln 2, n = 3, a = 1$ ).

The tests with discontinuous topology has a path on the maximum line also, the theoretical final state of a test can be identical to the global maximum of the normalized entropy increment  $B$  line if the fraction number becomes constant. This diagram point is the symmetry point of the upper bounding line of the normalized entropy diagram and the related grading curve has fractal dimension 3, independently of the number of fractions  $N$ .

If the starting point is on the left hand side of the diagram ( $A$  is less than  $1/2$ ), the normalised entropy path will be drifted to the right hand side of the diagram by the jump. Then the normalised entropy path may not reach the maximum  $B$  line at the right hand side of the diagram and its final point is uncertain.

## 5 CONCLUSION

1. The base entropy  $S_0$  decreases, and the entropy increment  $\Delta S$  strictly monotonically increases during breakage. This indicates that the breakage can be considered as a spontaneous process and,



that the entropy increment  $\Delta S$  can be related to the entropy principle of thermodynamics. The normalised entropy path is similar for constant fraction number. Its final point is dependent on the initial point and the type of the test.

2. If the number of the fractions changes (at the appearance of some finer fractions) temporarily a different, ‘opposite’ normalised entropy path may occur. The size of the measured ‘discontinuity’ seems to be directly related to  $1 - A$ , being zero if the starting point is a single fraction with  $A = 1$ , in accordance with the suggested formula. This means that a more stable state is the direction of the jump. The jump formula was supported by the measured data.
3. The results with silica and carbonate sands, and results with siltstone and andesite from the same initial grading and testing conditions, indicates the same normalized entropy paths are followed, only the rate of change is different. Since, by starting from the same initial grading, the normalized entropy path seems to be independent of the type of rock, there is potential to develop a new particle hardness test based on the entropy path followed during breakage.

## REFERENCES

1. Brandl, H. 1977. Ungebundene Tragschichten im Strassenbau Heft 67 Bundesministerium, Strassenforschung. 188p.
2. Coop, M. R., Sorensen, K. K., Bodas Freitas, K. K. & Georgoutsos, G. 2004. Particle breakage during shearing of a carbonate sand. *Geotechnique* 54(3): 157-163.
3. Dun, R. 2014 The Importance of Particle Breakage for Shear Strength Measured in Direct Shear. Undergraduate honours thesis. The School of Engineering. The University of Newcastle. (unpublished).
4. Einav, I (2007). “Breakage mechanics – Part I: Theory.” *J. of the Mech. and Physics of Solids*, Vol. 55, No. 3, pp. 1274-1297.
5. Imre E, Lőrincz J, Rózsa P, Trang Q P, 2008 Characterization of some sand mixtures. 12th International Conference on Computer Methods and Advances in Geomechanics. Goa, India, pp. 2064-2075.
6. Imre, E.; Lőrincz, J.; Trang, Q.P.; Fityus, S.; Pusztai, J.; Telekes, G.; Schanz, T. 2009 Some dry density transfer function for sands. *KSCE J. Civ. Eng.*, 13, 257–272.
7. Lőrincz, J; Imre, E; Gálos, M; Trang, Q.P; Telekes, G; Rajkai, K; Fityus, I. 2005 Grading entropy variation due to soil crushing. *Int. Journal. of Geomechanics*. Vol 5. Number 4. p. 311-320.
8. Lőrincz, J. 1986 On particle migration with the help of grading entropy. in *Filters in Geotechnical and Hydraulic Engineering*. Proceedings of the First International Conference on "Geo-Filters"
9. Lőrincz J, Imre E, Kárpáti L, Trang P Q, Fityus S. 2011 Some comments on the grading entropy variation and crushing of various sands. Proceedings of the 15th European Conference on Soil Mechanics and Geotechnical Engineering: Geotechnics. Athen, 2011.09.12-2011.09.15. Amsterdam: IOS Press, pp. 215-222. ISBN: 978-1-60750-800-7.

© 2015 by the authors; licensee MDPI, Basel, Switzerland. This article is an open access article distributed under the terms and conditions of the Creative Commons Attribution license (<http://creativecommons.org/licenses/by/3.0/>).